

Accepted Manuscript

Synthesis, antiameobic activity and docking studies of metronidazole-triazole-styryl hybrids

Beena Negi, Prija Poonan, Mohammad Fawad Ansari, Deepak Kumar, Sakshi Aggarwal, Ramandeep Singh, Amir Azam, Diwan S. Rawat



PII: S0223-5234(18)30276-9

DOI: [10.1016/j.ejmech.2018.03.033](https://doi.org/10.1016/j.ejmech.2018.03.033)

Reference: EJMECH 10298

To appear in: *European Journal of Medicinal Chemistry*

Received Date: 1 July 2017

Revised Date: 14 October 2017

Accepted Date: 12 March 2018

Please cite this article as: B. Negi, P. Poonan, M.F. Ansari, D. Kumar, S. Aggarwal, R. Singh, A. Azam, D.S. Rawat, Synthesis, antiameobic activity and docking studies of metronidazole-triazole-styryl hybrids, *European Journal of Medicinal Chemistry* (2018), doi: 10.1016/j.ejmech.2018.03.033.

This is a PDF file of an unedited manuscript that has been accepted for publication. As a service to our customers we are providing this early version of the manuscript. The manuscript will undergo copyediting, typesetting, and review of the resulting proof before it is published in its final form. Please note that during the production process errors may be discovered which could affect the content, and all legal disclaimers that apply to the journal pertain.

Synthesis, antiamoebic activity and docking studies of metronidazole-triazole-styryl hybrids

Beena Negi,^{a†} Prija Poonan,^a Mohammad Fawad Ansari,^b Deepak Kumar,^a Sakshi Aggarwal,^c Ramandeep Singh,^c Amir Azam,^b Diwan S Rawat^{a*}

^aDepartment of Chemistry, University of Delhi, Delhi 110007 (India)

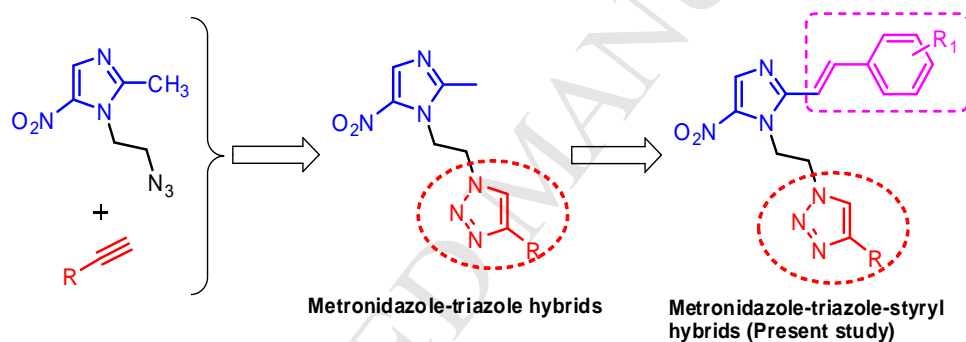
^bDepartment of Chemistry, Jamia Millia Islamia, Jamia Nagar, New Delhi (India)

^cTranslational Health Science and Technology Institute, Vaccine and Infectious Disease Research Centre, Faridabad-121001 (India)

[†]Current Address: Department of Chemistry, Gargi College, University of Delhi

*E-mail: dsrawat@chemistry.du.ac.in

Graphical Abstract



Synthesis, antiamoebic activity and docking studies of metronidazole-triazole-styryl hybrids

Beena Negi,^{a+} Prija Poonan,^a Mohammad Fawad Ansari,^b Deepak Kumar,^a Sakshi Aggarwal,^c Ramandeep Singh,^c Amir Azam,^b Diwan S Rawat^{a*}

^aDepartment of Chemistry, University of Delhi, Delhi 110007 (India)

^bDepartment of Chemistry, Jamia Millia Islamia, Jamia Nagar, New Delhi (India)

^cTranslational Health Science and Technology Institute, Vaccine and Infectious Disease Research Centre, Faridabad-121001(India)

⁺Current Address: Department of Chemistry, Gargi College, University of Delhi

*E-mail: dsrawat@chemistry.du.ac.in

Abstract: A series of 22 novel metronidazole-triazole-styryl hybrids were synthesized and evaluated for their *in vitro* antiamoebic activity against HM1: IMSS strain of *Entamoeba histolytica*. Some of the hybrids were found to be more active ($IC_{50} = 0.12 - 0.35 \mu M$) than the reference drug metronidazole ($IC_{50} = 1.79 \mu M$). The most active compounds were found to be non-toxic (up to $50 \mu M$) against the Vero cells showing a good safety profile of these hybrids. The docking and ADMET studies were also conducted to investigate the probable mode of action. Docking studies showed significant binding affinity in the active site of *E. histolytica* thioredoxin reductase (EhTrR) protein.

Key Words: metronidazole, triazole, *Entamoeba histolytica*, docking studies, thioredoxin reductase

*Corresponding author:

E. Mail: dsrawat@chemistry.du.ac.in

Phone No: 91-11-27662683

Fax No: 91-11-27667501

1. Introduction

Protozoan parasites have been causing serious problems to human health and are responsible for the high mortality and morbidity affecting more than 500 million people in the world [1]. Among protozoal infections, amoebiasis the third leading cause of death. It is caused by the protozoa *Entamoeba histolytica* which affects 50 million individuals per year [2]. The parasite affects the gastrointestinal tract of humans and causes invasive infections and induces tissue destruction, producing amoebic colitis, dysentery and liver abscesses [3].

The 5-nitroimidazole class of compounds has long been used for the treatment of protozoal infections. Among the nitroimidazole class of compounds, metronidazole (MTZ) is considered the drug of choice for the treatment of amoebiasis [4]. The nitro group in the metronidazole nucleus is crucial for its anti-amoebic activity. Reduction of the nitro group to the nitro radical anion by electron carriers in an anaerobic environment leads to decomposition to form toxic metabolites, which cause DNA damage and nonspecific macromolecular damage leading to cell death [5]. However, this drug is associated with certain serious side effects such as seizures, ataxia, gastric mucus irritation, genotoxicity, carcinogenicity spermatozoid damage and hematuria [6-10]. Moreover, there are reports of failure of treatment with metronidazole due to the development of resistance by the parasite towards MTZ [11,12]. Thus there is a need to develop novel anti-amoebic agents with increased efficacy and with no side effects. The two sites in the metronidazole moiety *viz.* the ethylhydroxy side chain and the methyl group attached to the imidazole ring, can be chemically modified to obtain a variety of compounds for the biological activity evaluation.

Recently the most promising and successful strategy to find a new drug is hybrid drug concept which involves covalent linking of two molecules with their individual activity into a single hybrid molecule [13]. In many cases the hybrid molecules have been found to have more potency towards both drug sensitive and resistant strains with better pharmacokinetic profile and less toxic effects [14-17]. Triazole moiety is one of the most widely studied pharmacophore showing a wide range of biological activities such as antibacterial, antiviral, antifungal, antitumor, anti-inflammatory and antiglycemic [18]. Considering the hybrid drug concept in our mind, we had synthesized some hybrid molecules bearing triazole nucleus in conjugation with the metronidazole (Fig. 1) which were found to exhibit remarkable anti-amoebic activities [19,20]. Encouraged by the anti-amoebic activity of MTZ-triazoles we designed and synthesised some novel metronidazole-triazole-styryl hybrids (Fig. 1).

Compounds containing styryl scaffold are known to possess wide spectrum of biological activities. The *trans*-cinnamic acid analogues have admirable pharmacological properties like antioxidant, antibacterial and antitumor [21]. Rubner *et al* had reported the cyanine-styryl-type dyes as bright non-covalent binders to RNA [22]. Hampannavar *et al* synthesised a series of styryl hydrazine thiazole hybrids and evaluated them *in vitro* against *M. tuberculosis* H37Rv strain [23]. Zaidi *et al* have reported antiamoebic activity of chalcones bearing *N*-substituted ethanamine tail, these compounds have C=C-Ph linkage in their structure [24]. Pais-Morales *et al* investigated the effect of resveratrol (a compound with C=C-Ph linkage) on *E. histolytica* trophozoites and the growth was arrested by 72 μ M dose level of resveratrol [25]. Abid *et al* have reported the synthesis of metronidazole thiosemicarbazone analogues with styryl linkage and one of the compounds showed promising antiamoebic activity at IC₅₀ 0.56 μ M [26]. Amalgamation of two biologically active pharmacophores (styryl and nitroimidazole) in one molecular platform generates a new scaffold for antiamoebic evaluation.

<Insert Fig. 1 here>

In order to understand the possible mechanism of action, molecular docking studies of the most active compounds were performed in the binding site of *E. histolytica* thioredoxin reductase (EhTrR) protein [27,28]. Leitsch *et al* identified five proteins, Trx, TrxR, SOD, purine nucleoside phosphorylase, and a protein with a carbohydrate binding domain that are affected by MTZ metabolites [29]. It has been shown that reduced MTZ binds covalently to TrxR and Trx in *E. histolytica*, which leads to inhibition of the physiological disulfide-reducing activity of the TrxR/Trx system. It has been suggested that the TrxR/Trx system is an excellent target for anti-parasite chemotherapy. In order to better understand Trx-dependent redox network of the parasite that could be indirectly affected by MTZ treatment, Schlosser *et al* screened the target proteome of Trx using an active site mutant (cysteine to serine) of Trx, which is capable of binding to interacting proteins but incapable to release its reduced targets.

2. Chemistry

The synthetic pathway leading to target compounds (**8-29**) is depicted in Scheme 1. Metronidazole (**1**) on reaction with *p*-toluene sulfonyl chloride yields tosyl derivative (**2**) which further on reaction with sodium azide gets converted to azide derivative (**3**). The azide derivative of MTZ on reaction with terminal alkynes yields MTZ-triazoles (**4-7**). Compounds

4-7 were treated with substituted benzaldehydes in presence of strong base to generate MTZ-triazole-styryl hybrids (**8-29**) (Scheme 1) [30]. The synthesized compounds were purified by column chromatography using 20% ethyl acetate : hexane as eluent.

<Insert Scheme 1 here>

3. Results and discussion

A series of 22 MTZ-triazole-styryl hybrids were evaluated *in vitro* for their anti-amoebic activity against HM1: IMSS strain of *E histolytica*. The MTZ-triazoles hybrids **4-7** have been reported earlier by our group and have IC₅₀ values 0.0223, 0.218, 0.0084 and 0.607 μM, respectively [20]. Modifications at the methyl group of these triazoles **4-7** led to the desired compounds **8-29** (Fig. 2). Modification of methyl group in compounds **4** (analogues **8-13**), **5** (analogues **14-19**) and **6** (analogues **20-24**) by styryl group resulted into compounds with decrease in activity, however the analogues **26** (4-F) and **27** (4-Cl) showed better activity than the parent compound **7**. This indicates that the incorporation of styryl group in place of methyl group is well tolerated.

<Insert Fig. 2 here>

Table 1 show that the *in vitro* activity of these hybrids was retained. Four different series of styryl derivatives (**8-13**, **14-19**, **20-24** and **25-29**) screened for *in vitro* antiamebic activity showed a similar trend in the activity due to the presence of various substituents on the phenyl ring. In the styryl derivatives of compounds **4**, **5**, **6** and **7** incorporation of polar groups like F, Cl and Br showed significant activity however a hydrophobic alkyl group such as methyl or ethyl leads to diminished activity.

Fourteen compounds (**8-11**, **14-17**, **21-23**, and **26-28**) were found to be more potent than the reference drug MTZ. Compounds **15** (IC₅₀ = 0.12 μM), **26** (IC₅₀ = 0.28 μM) and **27** (IC₅₀ = 0.35 μM) showed improved activity than the parent compounds **5** and **7**. The compounds **9**, **15**, **21** and **26** containing fluoro substituents were found to be more active than non-substituted analogues **8**, **14**, **20** and **25**, respectively. Replacement of F with Cl or Br leads to decrease in activity in compounds **10**, **11**, **16**, **17**, **22**, **23**, **27** and **28**, indicating significance of F towards biological activity of these compounds. However, compound **6** remains the most active compound amongst both the MTZ-triazole and MTZ-triazole-styryl series of compounds. Table 1 show that the change in the substituent present on the styryl moiety leads

to change in IC_{50} values of the compounds synthesized, which clearly indicates that the styryl linkage also plays a crucial role in the activity of these compounds.

Eleven compounds (**8-10**, **14-16**, **21-23**, **26** and **27**) with $IC_{50} > 1.35 \mu\text{M}$, were determined for cytotoxicity against Vero cell lines. The compounds tested were found to be non-toxic up to $50 \mu\text{M}$, highest tested concentration.

<Insert Table 1 here>

Molecular docking studies of the six most active MTZ-triazole-styryl hybrids having $IC_{50} < 1 \mu\text{M}$ (**9**, **15**, **21**, **22**, **26** and **27**) were performed in the NADP binding site of *E. histolytica* Thioredoxin reductase (EhTrR) (PDB ID:4CCQ) [32]. Thioredoxin reductase (TrR) prevents, regulates and repairs the damage caused by oxidative stress in *E. histolytica* [33]. Thioredoxin reductases enzymes are homodimeric proteins where each monomer contains a NADPH binding domain, FAD domain and an active site containing a redox active disulfide [34]. Thioredoxin reductase catalyzes the reversible transfer of reducing equivalents between NADPH and thioredoxin [35].

The results of docking studies for the test compounds are illustrated in Table 2. These docking results clearly indicate that the most active compounds in the study show substantial binding affinities towards EhTrR as exhibited by good Glide energy ($-52.48 \text{ kcalmol}^{-1}$ to $-43.84 \text{ kcalmol}^{-1}$) and GlideXP scores ($-6.51 \text{ kcalmol}^{-1}$ to $-5.29 \text{ kcalmol}^{-1}$). The docking conformations of the protein-ligand complexes having high Glide energy and GlideXP scores are presented in Figures 3 and 4 for compounds **15** and **21**, respectively. Figure 3 and 4 shows the hydrogen bonding pattern along with cation- π interactions and hydrophobic interactions of compounds **15** and **21** with the binding site residues. Interestingly, the compounds are showing H-bond interactions with the conserved residues of the coenzyme binding motif such as Arg183, Arg184, Arg188 and Gly160 similar to the native substrate NADP [36,37]. However, NADP being a bulky molecule could occupy a larger volume of the protein active site, hence forms several H-bond and hydrophobic interactions. This could be attributed for higher GlideXP score ($-9.43 \text{ kcalmol}^{-1}$) and Glide energy ($-73.86 \text{ kcalmol}^{-1}$) terms obtained for the docking results of NADP-EHTrR complex. Figure 3 shows the binding pose for **compound 15-EHTrR** complex. Side chains of Arg183 and Arg188 is forming H-bond interactions with the oxygen atom of nitro substituent of imidazole ring. Also side chain amine of Arg183 is forming cation- π interaction with the triazole ring of the compound.

Further main chain nitrogen of Gly 160 is involved in the H-bond interaction with imidazole nitrogen atom. 2D and 3D docking pose of **compound 21**-EHTrR complex (Fig. 4) shows the oxygen atoms of the nitro group of the compound forming H-bond interactions with side chain amine group of Arg183 and Arg184. The imidazole nitrogen of the compound forms H-bond with main chain nitrogen of Gly160. Further the π cloud of the triazole ring of the compound is involved in the cation- π interaction with the amine side chain of Arg183 (Fig. 4).

<Insert Table 2 here>

<Insert Fig. 3 here>

<Insert Fig. 4 here>

Lipinski's rule of five and pharmacokinetic data of these compounds were calculated through ADMET prediction using QikProp version 3.5. The most important of these parameters together with its permissible ranges are listed in the Tables 3 and 4. The active compounds were found to obey the Lipinski's rule of five, which is a preliminary test for drug-likeness of compounds. An orally active compound should not have more than 4 violations of Lipinski's Rule. Table 3 clearly indicates that all the compounds showed no violations of Lipinski's rule of 5.

With the exception of compound **27**, having $Q\text{PlogPo/w} > 5$, remaining compounds have good drug likeness properties (Table 4). Prediction of oral drug absorption (Percent Human Oral Absorption) was highly satisfactory for all the test compounds. QPPCaco predictions for all the test compounds showed high to moderately good values for Caco-2 cells permeability. Further, $Q\text{PlogKhsa}$, the prediction for human serum albumin binding and all inhibitors were predicted lie within the expected range for 95% of known drugs (-1.5 to 1.5). Also, the QikProp descriptor for brain/blood partition coefficient ($Q\text{PlogBB}$) and the blood-brain barrier mimic MDCK cell permeability ($Q\text{PPMDCK}$) show satisfactory predictions for all the test compounds and the reference compound. Further, aqueous solubility ($Q\text{PlogS}$) parameter for the test compounds were assessed and all the compounds were predicted to have $Q\text{PlogS}$ values in permissible range. Furthermore, $Q\text{PlogHERG}$ descriptor for the prediction of IC_{50} value of HERG K^+ channel blockage was predicted for the test compounds. With compound **23** ($Q\text{PlogHERG} = -4.863$) and for **MTZ** ($Q\text{PlogHERG} = -3.156$), having value in permissible limits, all other test compounds were having $Q\text{PlogHERG}$ descriptor below the recommended concerned value of -5.

<Insert Table 3 here>

<Insert Table 4 here>

4. Conclusion

The unification of nitroimidazole, styryl and triazole moieties is an effort to explore the influence of structural hybridizations on the activity, hoping to find a new lead structure that would have a promising antiamebic activity. The nitro group, imidazole, triazole and styryl contribute significantly towards the antiamebic activity. The MTZ-triazole and their novel styryl derivatives were effective against HM1: IMSS strain of *E histolytica*. Compound **6** (2-[1-[2-(2-Methyl-5-nitro-imidazol-1-yl)-ethyl]-1*H*-[1,2,3]triazol-4-yl]-pyridine) was found to be the most active against *E. Histolytica* amongst the MTZ-triazole series and MTZ-triazole-styryl hybrid series. Thus we strongly believe that compound **6** could be considered as a lead for the further development of anti-amebic agents.

5. Experimental Section

5.1. *In vitro* antiamebic activity

All the synthesized metronidazole-triazole-styryl hybrids (**8-29**) were screened for their *in vitro* antiamebic activity against HM1: IMSS strain of *E. histolytica* by microdilution method [31]. *E. histolytica* trophozoites were cultured in culture tubes by using Diamond TYIS-33 growth medium [38]. The test compounds (1mg) were dissolved in DMSO (40 μ L, level at which no inhibition of amoeba occurs) [39]. The stock solutions of the compounds were prepared freshly before use at a concentration of 1 mg/mL. Two-fold serial dilutions were made in the wells of 96-well microtiter plate. Each test includes MTZ as a standard amoebicidal drug, control wells (culture medium plus amoeba) and a blank (culture medium only). All the experiments were carried out in triplicate at each concentration level and repeated thrice. The amoeba suspension was prepared from a confluent culture by pouring off the medium at 37°C and adding 5 mL of fresh medium, chilling the culture tube on ice to detach the organisms from the side of flask. The number of amoeba/mL was estimated with the help of a haemocytometer, using trypan blue exclusion to confirm the viability. The suspension was diluted upto 10^5 organism/mL by adding fresh medium and 170 μ L of this suspension was added to the test and control wells in the plate so that the wells were completely filled (total volume, 340 μ L). An inoculum of 1.7×10^4 organisms/well was chosen so that confluent, but not excessive growth, took place in control wells. Plate was

sealed and gassed for 10 min with nitrogen before incubation at 37 °C for 72 h. After incubation, the growth of amoeba in the plate was checked with a low power microscope. The culture medium was removed by inverting the plate and shaking gently. Plate was then immediately washed with sodium chloride solution (0.9%) at 37 °C. This procedure was completed quickly and the plate was not allowed to cool in order to prevent the detachment of amoeba. The plate was allowed to dry at room temperature and the amoeba were fixed with methanol and when dried, stained with (0.5%) aqueous eosin for 15 min. The stained plate was washed once with tap water, then twice with distilled water and then allowed to dry. A 200 µL portion of 0.1 N sodium hydroxide solution was added to each well to dissolve the protein and release the dye. The optical density of the resulting solution in each well was determined at 490 nm with a microplate reader. The % inhibition of amoeba growth was calculated from the optical densities of the control and test wells and plotted against the logarithm of the dose of the drug tested. Linear regression analysis was used to determine the best fitting line from which the IC₅₀ value was found.

5.2 Molecular docking studies

The 2D structures of all the compounds were generated on ChemBioDraw Ultra 12.0 (www.cambridgesoft.com). Ligprep module implemented in Schrödinger was used to generate energy minimized 3D structures. Partial atomic charges were computed using the OPLS_2005 force field. The correct Lewis structure, tautomers and ionization states (pH 7.0 +/- 2.0) for each of these ligands were generated and optimized with default settings (Ligprep 2.5, Schrödinger, LLC, New York, NY, 2012). The 3D crystal structure of Thioredoxin reductase from *Entamoeba Histolytica* (PDB ID:4CCQ; resolution 1.50 Å), was retrieved from protein data bank (www.rcsb.org). The proteins were prepared for docking using Protein Preparation Wizard (Maestro 9.3 Schrödinger, LLC, New York, NY, 2012). Water molecules within 5 Å of the protein structures were considered. Bond order and formal charges were assigned and hydrogen atoms were added to the crystal structure. Further to refine the structure OPLS-2005 force field parameter was used to alleviate steric clashes and the minimization was terminated when RMSD reached maximum cut off value of 0.30 Å. The binding site was defined by a 20 Å × 20 Å × 20 Å box centered on the centroid of the EHTrR natural substrate, NADP as the centroid of the ligands used for docking. Default settings were used for all the remaining parameters and no constraints were specified separately. All ligand conformers were docked to each of the receptor grid files EHTrR

structures using Glide extra precision (XP) mode. Default settings were used for the refinement and scoring.

5.3 *In silico* ADMET Prediction

The pharmacokinetic profile of compounds in the study were predicted by using programs Qikprop v3.5 (Schrödinger, Inc., New York, NY, 2012) [40]. All the compounds were prepared in neutralized form for the calculation of pharmacokinetic properties by QikProp using Schrodinger's Maestro Build module and LigPrep, saved in SD format. The programs QikProp utilizes the method of Jorgensen [41] to compute pharmacokinetic properties and descriptors such as octanol/water partitioning coefficient, aqueous solubility, brain/blood partition coefficient, intestinal wall permeability, plasma protein binding etc.

5.4 Synthetic Methodology

All the chemicals were purchased from Sigma-Aldrich and were used without further purification. Progress of the reactions was monitored by thin layer chromatography (Merck Kiesel 60 F254, 0.2 mm thickness) and the compounds were purified by silica gel column chromatography. IR spectra were recorded on Perkin-elmer FT-IR spectrophotometer using KBr pellets and the values were expressed in cm^{-1} . ^1H NMR (400 MHz) and ^{13}C NMR (100 MHz) spectra were recorded on Jeol ECX spectrospin instrument using CDCl_3 or $\text{DMSO-}d_6$ as solvent with TMS as internal reference. The chemical shift values were expressed on δ scale and the coupling constant (J) in Hz. Melting points were recorded on EZ-Melt automated melting point apparatus, Stanford Research Systems and are uncorrected. Mass data were recorded in Jeol-Accu TOF JMS-T100LC and micromass LCT mass spectrometer/Data system.

5.5 Typical procedure for the synthesis of (E)-(1-(2-(5-Nitro-2-styryl-1H-imidazol-1-yl)ethyl)-1H-1,2,3-triazol-4-yl)methanol (8) and related compounds (8-29): To a stirred solution of compound **6** (200 mg, 0.609 mmol) in DMSO (5 mL) benzaldehyde (64.6 mg, 0.609 mmol) or substituted benzaldehydes was added. The reaction mixture was cooled to 0 °C and a solution sodium methoxide (98.7 mg, 1.829 mmol) in dry MeOH (5 mL) was added. The reaction mixture was further stirred at 40 °C for 12 h. The solid obtained was filtered and purified by column chromatography to obtain compound **8-29**.

5.5.1. (E)-(1-(2-(5-Nitro-2-styryl-1H-imidazol-1-yl)ethyl)-1H-1,2,3-triazol-4-yl)methanol (8): Yield 56%; mp 161-162 °C; IR (film, cm^{-1}): 2923, 2857, 1625, 1429, 1377, 1263, 1190,

1032; ^1H NMR (400 MHz, DMSO- d_6) δ : 4.23 (d, $J = 5.8$ Hz, 2H, CH_2OH), 4.81 (t, $J = 5.1$ Hz, 2H, NCH_2), 4.98 (t, $J = 5.8$ Hz, 2H, NCH_2), 5.06 (t, $J = 5.8$ Hz, 1H, CH_2OH), 6.60 (d, $J = 16.1$ Hz, 1H, $\text{CH}=\text{CH}$), 7.36-7.39 (m, 2H, ArH), 7.41-7.43 (m, 1H), 7.56 (d, $J = 15.4$ Hz, 1H, $\text{CH}=\text{CH}$), 7.60 (d, $J = 6.6$ Hz, 2H, ArH), 7.90 (s, 1H), 8.22 (s, 1H); ^{13}C NMR (100 MHz, DMSO- d_6) δ : 45.24, 49.02, 54.83, 112.01, 123.55, 127.65, 128.75, 129.43, 134.99, 135.27, 138.22, 138.51, 148.27, 150.16; ESI-MS (m/z): 341.34 $[\text{M} + \text{H}]^+$. Anal Calcd for $\text{C}_{16}\text{H}_{16}\text{N}_6\text{O}_3$: C 56.47, H 4.74, N 24.69. Found: C 56.65, H 4.90, N 24.82.

5.5.2. (E)-(1-(2-(2-(4-Fluorostyryl)-5-nitro-1H-imidazol-1-yl)ethyl)-1H-1,2,3-triazol-4-yl) methanol (9): Yield 57%; mp 160-162 $^\circ\text{C}$; IR (film, cm^{-1}): 2922, 2852, 1443, 1380, 1278, 1184, 970, 821, 764; ^1H NMR (400 MHz, CDCl_3) δ : 3.85 (s, 1H, OH), 4.58 (d, $J = 3.6$ Hz, 2H, CH_2OH), 4.86-4.87 (m, 2H, NCH_2), 4.93-4.97 (m, 2H, NCH_2), 5.95 (d, $J = 15.4$ Hz, 1H, $\text{CH}=\text{CH}$), 6.93 (d, $J = 8$ Hz, 2H, ArH), 7.08-7.13 (m, 1H, ArH), 7.41-7.45 (m, 2H, ArH), 7.69 (d, $J = 15.4$ Hz, 1H, $\text{CH}=\text{CH}$), 8.15 (s, 1H); ESI-MS (m/z): 359.28 $[\text{M} + \text{H}]^+$. Anal Calcd for $\text{C}_{16}\text{H}_{15}\text{FN}_6\text{O}_3$: C 53.63, H 4.22, N 23.45. Found: C 53.46, H 4.12, N 23.61.

5.5.3. (E)-(1-(2-(2-(4-Chlorostyryl)-5-nitro-1H-imidazol-1-yl)ethyl)-1H-1,2,3-triazol-4-yl) methanol (10): Yield 51%; mp 221-222 $^\circ\text{C}$; IR (film, cm^{-1}): 2919, 2850, 1433, 1380, 1264, 1226, 1189, 1091, 1007, 968, 813; ^1H NMR (400 MHz, CDCl_3) δ : 1.72 (t, $J = 5.9$ Hz, 1H, CH_2OH), 4.59 (d, $J = 6.6$ Hz, 2H, CH_2OH), 4.85 (t, $J = 5.9$ Hz, 2H, NCH_2), 4.96 (t, $J = 5.9$ Hz, 2H, NCH_2), 6.10 (d, $J = 15.4$ Hz, 1H, $\text{CH}=\text{CH}$), 7.25 (s, 1H), 7.39 (dd, $J = 8.8$ Hz, 2.9 Hz, 4H, ArH), 7.68 (d, $J = 15.4$ Hz, 1H, $\text{CH}=\text{CH}$), 8.15 (s, 1H); ESI-MS (m/z): 375.22 $[\text{M} + \text{H}]^+$, 377.24 $[\text{M} + 2]^+$. Anal Calcd for $\text{C}_{16}\text{H}_{15}\text{ClN}_6\text{O}_3$: C 51.28, H 4.03, N 22.42. Found: C 51.39, H 4.14, N 22.33.

5.5.4. (E)-(1-(2-(2-(4-Bromostyryl)-5-nitro-1H-imidazol-1-yl)ethyl)-1H-1,2,3-triazol-4-yl) methanol (11): Yield 61%; mp 222-223 $^\circ\text{C}$; IR (film, cm^{-1}): 2921, 1623, 1420, 1027, 996; ^1H NMR (400 MHz, CDCl_3) δ : 1.71 (t, $J = 5.9$ Hz, 1H, CH_2OH), 4.59 (d, $J = 5.9$ Hz, 2H, CH_2OH), 4.85 (t, $J = 5.9$ Hz, 2H, NCH_2), 4.96 (t, $J = 5.9$ Hz, 2H, NCH_2), 6.12 (d, $J = 15.4$ Hz, 1H, $\text{CH}=\text{CH}$), 7.25 (s, 1H), 7.33 (d, $J = 8.8$ Hz, 2H, ArH), 7.54 (d, $J = 8.0$ Hz, 2H, ArH), 7.66 (d, $J = 15.4$ Hz, 1H, $\text{CH}=\text{CH}$), 8.14 (s, 1H); ESI-MS (m/z): 419.12 $[\text{M} + \text{H}]^+$, 421.14 $[\text{M} + 2]^+$. Anal calcd for $\text{C}_{16}\text{H}_{15}\text{BrN}_6\text{O}_3$: C 45.84, H 3.61, N 20.05. Found: C 45.96, H 3.52, N 20.16.

5.5.5. (E)-1-(2-(2-(4-Methylstyryl)-5-nitro-1H-imidazol-1-yl)ethyl)-1H-1,2,3-triazol-4-yl methanol (12): Yield 59%; mp 200-201 °C; ¹H NMR (400 MHz, DMSO-*d*₆) δ: 2.32 (s, 3H, CH₃), 4.23 (d, *J* = 5.8 Hz, 2H, CH₂OH), 4.80 (t, *J* = 5.8 Hz, 2H, NCH₂), 4.96 (t, *J* = 5.8 Hz, 2H, NCH₂), 5.06 (t, *J* = 5.8 Hz, 1H, CH₂OH), 6.54 (d, *J* = 15.4 Hz, 1H, CH=CH), 7.21 (d, *J* = 8 Hz, 2H, ArH), 7.49 (d, *J* = 8 Hz, 2H, ArH), 7.52 (d, *J* = 16.1 Hz, 1H, CH=CH), 7.89 (s, 1H), 8.20 (s, 1H); ¹³C NMR (100 MHz, DMSO-*d*₆) δ: 21.00, 45.18, 49.00, 54.83, 110.91, 123.51, 127.63, 129.34, 132.55, 135.05, 138.29, 138.42, 139.25, 148.24, 150.39; ESI-MS (*m/z*): 355.26 [M + H]⁺. Anal calcd for C₁₇H₁₈N₆O₃: C 57.62, H 5.12, N, 23.72. Found: C 57.73, H 5.02, N, 23.59.

5.5.6. (E)-1-(2-(2-(4-Ethylstyryl)-5-nitro-1H-imidazol-1-yl)ethyl)-1H-1,2,3-triazol-4-yl methanol (13): Yield 48%; mp 180-181 °C; IR (film, cm⁻¹): 2920, 2850, 1458, 1378, 1263, 1189, 1219, 1032; ¹H NMR (400 MHz, CDCl₃) δ: 1.25 (t, *J* = 7.0 Hz, 3H, CH₂CH₃), 1.66 (t, *J* = 5.9 Hz, 1H, CH₂OH), 2.68 (q, *J* = 7.3 Hz, 2H, CH₂CH₃), 4.58 (d, *J* = 5.9 Hz, 2H, CH₂OH), 4.85 (t, *J* = 5.1 Hz, 2H, NCH₂), 4.95 (t, *J* = 5.1 Hz, 2H, NCH₂), 6.08 (d, *J* = 15.4 Hz, 1H, CH=CH), 7.23 (s, 1H), 7.26 (s, 2H, ArH), 7.39 (d, *J* = 8.0 Hz, 2H, ArH), 7.72 (d, *J* = 15.4 Hz, 1H, CH=CH), 8.15 (s, 1H); ESI-MS (*m/z*): 369.28 [M + H]⁺. Anal calcd for C₁₈H₂₀N₆O₃: C 58.69, H 5.47, N 22.81

5.5.7. (E)-1-(2-(5-Nitro-2-styryl-1H-imidazol-1-yl)ethyl)-4-phenyl-1H-1,2,3-triazole (14): Yield 63%; mp 230-231 °C; IR (film, cm⁻¹): 2922, 1440, 1380, 1261, 1187; ¹H NMR (400 MHz, CDCl₃) δ: 4.91 (t, *J* = 5.1 Hz, 2H, NCH₂), 4.99 (t, *J* = 5.1 Hz, 2H, NCH₂), 6.20 (d, *J* = 15.4 Hz, 1H, CH=CH), 7.25 (s, 1H, ArH), 7.29 (s, 1H, ArH), 7.30 (s, 1H, ArH), 7.32-7.35 (m, 3H, ArH), 7.39-7.41 (m, 2H, ArH), 7.49 (s, 1H), 7.55-7.57 (m, 2H, ArH), 7.67 (d, *J* = 15.4 Hz, 1H, CH=CH), 8.16 (s, 1H); ESI-MS (*m/z*): 387.25 [M + H]⁺. Anal calcd for C₂₁H₁₈N₆O₂: C 65.27, H 4.70, N 21.75. Found: C 65.39, H 4.59, N 21.87.

5.5.8. (E)-1-(2-(2-(4-Fluorostyryl)-5-nitro-1H-imidazol-1-yl)ethyl)-4-phenyl-1H-1,2,3-triazole (15): Yield 53%; mp 181-182 °C; IR (film, cm⁻¹): 3119, 3089, 2920, 1598, 1518, 1487, 1449, 1381, 1273, 1261, 1227, 1187, 1039; ¹H NMR (400 MHz, CDCl₃) δ: 4.91-4.92 (m, 2H, NCH₂), 4.96-5.0 (m, 2H, NCH₂), 6.05 (d, *J* = 15.4 Hz, 1H, CH=CH), 7.30 (d, *J* = 7.3 Hz, 1H, ArH), 7.34-7.37 (m, 2H, ArH), 7.42-7.45 (m, 2H, ArH), 7.48 (d, *J* = 8 Hz, 1H, ArH), 7.54-7.56 (m, 1H, ArH), 7.60 (d, *J* = 15.4 Hz, 1H, CH=CH), 7.40-7.76 (m, 2H, ArH), 8.03 (s, 1H), 8.15 (s, 1H); ESI-MS (*m/z*): 405.28 [M + H]⁺. Anal calcd for C₂₁H₁₇FN₆O₂: C 62.37, H 4.24, N 20.78. Found: C 62.48, H 4.33, N 20.65.

5.5.9. *(E)-1-(2-(2-(4-Chlorostyryl)-5-nitro-1H-imidazol-1-yl)ethyl)-4-phenyl-1H-1,2,3-triazole (16)*: Yield 38%; mp 272-273 °C; IR (film, cm⁻¹): 3085, 2922, 2852, 1519, 1485, 1449, 1433, 1378, 1271, 1259, 1187, 1178, 1086, 1011; ¹H NMR (400 MHz, DMSO-*d*₆) δ: 4.87 (t, *J* = 5.8 Hz, 2H, NCH₂), 5.03 (t, *J* = 5.1 Hz, 2H, NCH₂), 6.64 (d, *J* = 15.4 Hz, 1H, CH=CH), 7.23-7.25 (m, 1H), 7.26 (s, 1H, ArH), 7.28-7.30 (m, 2H, ArH), 7.31 (s, 1H, ArH), 7.44 (d, *J* = 16.1 Hz, 1H, CH=CH), 7.49-7.50 (m, 2H), 7.52-7.53 (m, 2H), 8.22 (s, 1H), 8.44 (s, 1H); ¹³C NMR (100 MHz, DMSO-*d*₆) δ: 45.26, 49.41, 112.22, 122.22, 125.03, 127.68, 128.52, 128.62, 129.18, 130.34, 133.70, 134.01, 135.05, 136.73, 138.54, 146.62, 149.97; ESI-MS (*m/z*): 421.28 [M + H]⁺, 423.29 [M + 2]⁺. Anal calcd for C₂₁H₁₇ClN₆O₂: C 59.93, H 4.07, N 19.97. Found: C 59.83, H 4.18, N 19.88.

5.5.10. *(E)-1-(2-(2-(4-Bromostyryl)-5-nitro-1H-imidazol-1-yl)ethyl)-4-phenyl-1H-1,2,3-triazole (17)*: Yield 64%; mp 270-271 °C; IR (film, cm⁻¹): 3409, 3111, 3083, 2922, 1521, 1487, 1450, 1431, 1381, 1271, 1199, 1073; ¹H NMR (400 MHz, DMSO-*d*₆) δ: 4.88 (t, *J* = 5.1 Hz, 2H, NCH₂), 5.04 (t, *J* = 5.8 Hz, 2H, NCH₂), 6.66 (d, *J* = 16.1 Hz, 1H, CH=CH), 7.24-7.27 (m, 1H), 7.29-7.31 (m, 1H, ArH), 7.43 (d, *J* = 15.4 Hz, 1H, CH=CH), 7.44 (s, 5H, ArH), 7.50-7.51 (m, 1H), 7.52-7.53 (m, 1H), 8.24 (s, 1H), 8.44 (s, 1H); ¹³C NMR (100 MHz, DMSO-*d*₆) δ: 45.28, 49.42, 112.69, 122.22, 122.51, 125.04, 127.68, 128.63, 129.42, 130.34, 131.45, 134.34, 135.06, 136.81, 138.55, 146.63, 149.97; ESI-MS (*m/z*): 467.24 [M + H]⁺, 469.26 [M + 2]⁺. Anal calcd for C₂₁H₁₇BrN₆O₂: C 54.21, H 3.68, N 18.06. Found: C 54.33, H 3.59, N 18.19.

5.5.11. *(E)-1-(2-(2-(4-Methylstyryl)-5-nitro-1H-imidazol-1-yl)ethyl)-4-phenyl-1H-1,2,3-triazole (18)*: Yield 51%; mp 237-238 °C; IR (film, cm⁻¹): 3082, 1516, 1449, 1430, 1378, 1275, 1260, 1176, 1199; ¹H NMR (400 MHz, DMSO-*d*₆) δ: 2.29 (s, 3H, CH₃), 4.88 (t, *J* = 5.8 Hz, 2H, NCH₂), 5.03 (t, *J* = 5.8 Hz, 2H, NCH₂), 6.58 (d, *J* = 16.1 Hz, 1H, CH=CH), 7.10 (d, *J* = 8 Hz, 2H, ArH), 7.24-7.62 (m, 1H, ArH), 7.28-7.32 (m, 2H), 7.41 (d, *J* = 8 Hz, 2H, ArH), 7.47 (d, *J* = 15.4 Hz, 1H, CH=CH), 7.54 (s, 1H, ArH), 7.56 (d, *J* = 1.5 Hz, 1H, ArH), 8.22 (s, 1H), 8.46 (s, 1H); ¹³C NMR (100 MHz, DMSO-*d*₆) δ: 20.99, 45.20, 49.41, 110.79, 122.24, 125.13, 127.59, 127.70, 128.67, 129.20, 130.42, 132.40, 135.16, 138.48, 139.17, 146.64, 150.47; ESI-MS (*m/z*): 401.28 [M + H]⁺. Anal calcd for C₂₂H₂₀N₆O₂: C 65.99, H 5.03, N 20.99. Found: C 65.89, H 5.14, N 20.88.

5.5.12. *(E)-1-(2-(2-(4-Ethylstyryl)-5-nitro-1H-imidazol-1-yl)ethyl)-4-phenyl-1H-1,2,3-triazole (19)*: Yield 56%; mp 230-231 °C; IR (film, cm⁻¹): 3081, 2924, 1448, 1384, 1272,

1182; ^1H NMR (400 MHz, DMSO- d_6) δ : 1.15 (t, J = 7.3 Hz, 3H, CH_2CH_3), 2.57 (q, J = 7.3 Hz, 2H, CH_2CH_3), 4.88 (t, J = 5.9 Hz, 2H, NCH_2), 5.02 (t, J = 5.9 Hz, 2H, NCH_2), 6.56 (d, J = 15.4 Hz, 1H, $\text{CH}=\text{CH}$), 7.11 (d, J = 8.0 Hz, 2H, ArH), 7.21-7.25 (m, 1H, ArH), 7.27-7.31 (m, 2H, ArH), 7.41 (d, J = 8.0 Hz, 2H, ArH), 7.47 (d, J = 15.4 Hz, 1H, $\text{CH}=\text{CH}$), 7.54 (s, 1H), 7.56 (d, J = 1.5 Hz, 1H, ArH), 8.22 (s, 1H), 8.47 (s, 1H); ^{13}C NMR (100 MHz, DMSO- d_6) δ : 15.38, 28.02, 45.23, 49.42, 110.84, 122.23, 125.13, 127.67, 127.99, 128.65, 130.42, 132.64, 135.15, 144.41, 146.65, 150.46; ESI-MS (m/z): 415.32 $[\text{M} + \text{H}]^+$. Anal calcd for $\text{C}_{23}\text{H}_{22}\text{N}_6\text{O}_2$: C 66.65, H 5.35, N 20.28. Found C 66.61, H 5.32, N 20.22.

5.5.13. (*E*)-2-(1-(2-(5-Nitro-2-styryl-1H-imidazol-1-yl)ethyl)-1H-1,2,3-triazol-4-yl)pyridine (**20**): Yield 62%; mp 208-209 °C; IR (film, cm^{-1}): 3076, 2920, 2851, 1603, 1518, 1490, 1461, 1446, 1428, 1378, 1304, 1260, 1190, 1157, 1081, 1038, 996, 961, 821, 784; ^1H NMR (400 MHz, CDCl_3) δ : 4.93 (t, J = 5.1 Hz, 2H, NCH_2), 5.00 (t, J = 5.1 Hz, 2H, NCH_2), 6.20 (d, J = 15.4 Hz, 1H, $\text{CH}=\text{CH}$), 7.15-7.18 (m, 1H, ArH), 7.30-7.32 (m, 3H, ArH), 7.36-7.38 (m, 2H, ArH), 7.59-7.61 (m, 1H, ArH), 7.65 (d, J = 15.4 Hz, 1H, $\text{CH}=\text{CH}$), 7.84 (d, J = 8.0 Hz, 1H, ArH), 7.94 (s, 1H, ArH), 8.16 (s, 1H), 8.49 (d, J = 3.7 Hz, 1H, ArH); ESI-MS (m/z): 388.26 $[\text{M} + \text{H}]^+$. Anal calcd for $\text{C}_{20}\text{H}_{17}\text{N}_7\text{O}_2$: C 62.01, H 4.42, N 25.31. Found: C 62.06, H 4.45, N 25.28.

5.5.14. (*E*)-2-(1-(2-(2-(4-Fluorostyryl)-5-nitro-1H-imidazol-1-yl)ethyl)-1H-1,2,3-triazol-4-yl)pyridine (**21**): Yield 32%; mp 188-189 °C; IR (film, cm^{-1}): 2927, 1596, 1508, 1420, 1363, 1259, 1227, 1188, 1080, 1036; ^1H NMR (400 MHz, CDCl_3) δ : 4.92-4.94 (m, 2H, NCH_2), 4.98-5.0 (m, 2H, NCH_2), 6.06 (d, J = 15.4 Hz, 1H, $\text{CH}=\text{CH}$), 6.96-7.0 (m, 1H, ArH), 7.16-7.19 (m, 1H, ArH), 7.32-7.36 (m, 2H, ArH), 7.58 (d, J = 15.4 Hz, 1H, ArH), 7.62-7.65 (m, 1H, ArH), 7.83-7.87 (m, 1H, ArH), 7.91 (s, 1H), 7.94 (d, J = 4.4 Hz, 1H, ArH), 8.15 (s, 1H), 8.55-8.56 (m, 1H, ArH); ESI-MS (m/z): 406.30 $[\text{M} + \text{H}]^+$. Anal calcd for $\text{C}_{20}\text{H}_{16}\text{FN}_7\text{O}_2$: C 59.26, H 3.98, N 24.19. Found: C 59.35, H 3.88, N 24.28.

5.5.15. (*E*)-2-(1-(2-(2-(4-Chlorostyryl)-5-nitro-1H-imidazol-1-yl)ethyl)-1H-1,2,3-triazol-4-yl)pyridine (**22**): Yield 80%; mp 210-211 °C; ^1H NMR (400 MHz, CDCl_3) δ : 4.92-4.94 (m, 2H, NCH_2), 4.98-4.99 (m, 2H, NCH_2), 6.10 (d, J = 15.4 Hz, 1H, $\text{CH}=\text{CH}$), 7.17-7.20 (m, 2H, ArH), 7.29 (s, 1H), 7.56 (d, J = 15.4 Hz, 1H, $\text{CH}=\text{CH}$), 7.61-7.65 (m, 1H, ArH), 7.82-7.84 (m, 1H, ArH), 7.91-7.95 (m, 1H, ArH), 8.07 (s, 1H), 8.14-8.16 (m, 1H, ArH), 8.48-8.49 (m, 1H, ArH), 8.55-8.56 (m, 1H, ArH); ESI-MS (m/z): 422.25 $[\text{M} + \text{H}]^+$, 444.28 $[\text{M} + \text{H}]^+$. Anal calcd for $\text{C}_{20}\text{H}_{16}\text{ClN}_7\text{O}_2$: C 56.94, H 3.82, N 23.24. Found: C 56.83, H 3.92, N 23.35.

5.5.16. *(E)-2-(1-(2-(2-(4-Bromostyryl)-5-nitro-1H-imidazol-1-yl)ethyl)-1H-1,2,3-triazol-4-yl)pyridine (23)*: Yield 40%; mp 212-213 °C; IR (film, cm⁻¹): 3369, 3131, 3086, 1597, 1535, 1524, 1458, 1448, 1379, 1269, 1232, 1079; ¹H NMR (400 MHz, CDCl₃) δ: 4.92-4.93 (m, 2H, NCH₂), 4.98-4.99 (m, 2H, NCH₂), 6.11 (d, *J* = 15.4 Hz, 1H, CH=CH), 7.20 (d, *J* = 8 Hz, 3H, ArH), 7.41 (d, *J* = 8 Hz, 2H, ArH), 7.54 (d, *J* = 15.4 Hz, 1H, CH=CH), 7.62-7.66 (m, 1H, ArH), 7.82 (d, *J* = 8 Hz, 1H, ArH), 7.93 (s, 1H), 8.15 (s, 1H), 8.48 (d, *J* = 2.9 Hz, 1H, ArH); ESI-MS (*m/z*): 466.23 [M + H]⁺, 468.28 [M + 2]⁺. Anal calcd for: C₂₀H₁₆BrN₇O₂: C 51.52, H 3.46, N 21.03. Found: C 51.56, H 3.41, N 21.11.

5.5.17. *(E)-2-(1-(2-(2-(4-Methylstyryl)-5-nitro-1H-imidazol-1-yl)ethyl)-1H-1,2,3-triazol-4-yl)pyridine (24)*: Yield 58%; mp 237-238 °C; IR (film, cm⁻¹): 3087, 2916, 2848, 1596, 1516, 1485, 1443, 1379, 1361, 1265, 1227, 1194, 1082, 1038, 996; ¹H NMR (400 MHz, CDCl₃) δ: 2.35 (s, 3H, CH₃), 4.92 (t, *J* = 5.9 Hz, 2H, NCH₂), 4.99 (t, *J* = 5.9 Hz, 2H, NCH₂), 6.17 (d, *J* = 15.4 Hz, 1H, CH=CH), 7.11 (d, *J* = 8.0 Hz, 2H, ArH), 7.15-7.18 (m, 1H), 7.28 (d, *J* = 8 Hz, 2H, ArH), 7.60-7.62 (m, 1H), 7.65 (s, 1H), 7.85 (d, *J* = 6.6 Hz, 1H, ArH), 7.94 (s, 1H), 8.15 (s, 1H), 8.49 (d, *J* = 3 Hz, 1H, ArH); ¹³C NMR (100 MHz, CDCl₃) δ: 21.47, 45.88, 50.11, 108.34, 120.18, 122.96, 123.09, 127.66, 129.50, 131.99, 135.51, 136.72, 140.29, 141.45, 149.12, 149.30, 149.39, 151.21; ESI-MS (*m/z*): 402.25 [M + H]⁺. Anal calcd for C₂₁H₁₉N₇O₂: C 62.83, H 4.77, N 24.42. Found: C 62.80, H 4.71, N 24.46.

5.5.18. *(E)-1-(2-(5-nitro-2-styryl-1H-imidazol-1-yl)ethyl)-4-(phenoxymethyl)-1H-1,2,3-triazole (25)*: Yield 47%; mp 179-180 °C; IR (film, cm⁻¹): 2923, 2852, 1491, 1459, 1429, 1379, 1264, 1243, 1192, 1050; ¹H NMR (400 MHz, CDCl₃) δ: 4.87 (t, *J* = 5.1 Hz, 2H, NCH₂), 4.97 (t, *J* = 5.1 Hz, 2H, NCH₂), 4.99 (s, 2H, OCH₂), 6.18 (d, *J* = 15.4 Hz, 1H, CH=CH), 6.82 (d, *J* = 7.3 Hz, 2H, ArH), 6.92-6.96 (m, 1H, ArH), 7.21-7.25 (m, 2H, ArH), 7.36-7.42 (m, 4H, ArH), 7.46-7.48 (m, 2H, ArH), 7.75 (d, *J* = 15.4 Hz, 1H, CH=CH), 8.15 (s, 1H); ESI-MS (*m/z*): 417.32 [M + H]⁺. Anal calcd for C₂₂H₂₀N₆O₃: C 63.45, H 4.84, N 20.18. Found: C 63.41, H 4.80, N 20.12.

5.5.19. *(E)-1-(2-(2-(4-Fluorostyryl)-5-nitro-1H-imidazol-1-yl)ethyl)-4-(phenoxymethyl)-1H-1,2,3-triazole (26)*: Yield 44%; mp 182-183 °C; IR (film, cm⁻¹): 2921, 2851, 1449, 1379, 1254, 1192, 1173, 1032; ¹H NMR (400 MHz, CDCl₃) δ: 4.87-4.88 (m, 2H, NCH₂), 4.93-4.97 (m, 2H, NCH₂), 5.0 (s, 2H, OCH₂), 6.07 (d, *J* = 15.4 Hz, 1H, CH=CH), 6.81-6.84 (m, 2H, ArH), 6.90-6.96 (m, 2H, ArH), 7.08 (s, 1H), 7.22 (d, *J* = 8.8 Hz, 2H, ArH), 7.36 (d, *J* = 7.3 Hz, 1H, ArH), 7.42 (d, *J* = 8.8 Hz, 1H, ArH), 7.45-7.47 (m, 1H, ArH), 7.69 (d, *J* = 15.4 Hz, 1H,

$CH=CH$), 8.14 (s, 1H); ESI-MS (m/z): 435.27 [$M + H$]⁺. Anal calcd for $C_{22}H_{19}FN_6O_3$: C 60.82, H 4.41, N 19.35. Found: C 60.93, H 4.55, N 19.44.

5.5.20. (E)-1-(2-(2-(4-Chlorostyryl)-5-nitro-1H-imidazol-1-yl)ethyl)-4-(phenoxyethyl)-1H-1,2,3-triazole (27): Yield 51%; mp 211-212 °C; IR (film, cm^{-1}): 3079, 2918, 2850, 1450, 1383, 1271, 1243, 1194, 1172, 1049; ¹H NMR (400 MHz, $CDCl_3$) δ : 4.86 (t, $J = 5.8$ Hz, 2H, NCH_2), 4.97 (t, $J = 5.1$ Hz, 2H, NCH_2), 4.99 (s, 2H, OCH_2), 6.12 (d, $J = 15.4$ Hz, 1H, $CH=CH$), 6.82 (d, $J = 8$ Hz, 2H, ArH), 6.94 (t, $J = 7.3$ Hz, 1H), 7.22 (d, $J = 7.3$ Hz, 2H, ArH), 7.35 (d, $J = 5.8$ Hz, 3H, ArH), 7.39 (d, $J = 8$ Hz, 2H, ArH), 7.67 (d, $J = 15.4$ Hz, 1H, $CH=CH$), 8.14 (s, 1H); ESI-MS (m/z): 451.23 [$M + H$]⁺, 453.24 [$M + 2$]⁺. Anal calcd for $C_{22}H_{19}ClN_6O_3$: C 58.60, H 4.25, N 18.64. Found: C 58.72, H 4.37, N 18.57.

5.5.21. (E)-1-(2-(2-(4-Bromostyryl)-5-nitro-1H-imidazol-1-yl)ethyl)-4-(phenoxyethyl)-1H-1,2,3-triazole (28): Yield 52%; mp 223-224 °C; IR (film, cm^{-1}): 2921, 2851, 1516, 1458, 1377, 1263, 1181, 1059, 970; ¹H NMR (400 MHz, $CDCl_3$) δ : 4.86 (t, $J = 5.8$ Hz, 2H, NCH_2), 4.96 (t, $J = 5.8$ Hz, 2H, NCH_2), 4.99 (s, 2H, OCH_2), 6.15 (d, $J = 16.1$ Hz, 1H, $CH=CH$), 6.82 (d, $J = 7.3$ Hz, 2H, ArH), 6.92-6.96 (m, 1H, ArH), 7.22 (d, $J = 7.3$ Hz, 2H, ArH), 7.31 (s, 1H), 7.33 (d, $J = 3.7$ Hz, 2H, ArH), 7.50 (s, 1H), 7.52 (d, $J = 1.5$ Hz, 1H, ArH), 7.65 (d, $J = 15.4$ Hz, 1H, $CH=CH$), 8.13 (s, 1H); ESI-MS (m/z): 495.18 [$M + H$]⁺, 497.17 [$M + 2$]⁺. Anal calcd for $C_{22}H_{19}BrN_6O_3$: C 53.35, H 3.87, N 16.97. Found: C 53.32, H 3.81, N 16.90.

5.5.22. (E)-1-(2-(2-(4-Methylstyryl)-5-nitro-1H-imidazol-1-yl)ethyl)-4-(phenoxyethyl)-1H-1,2,3-triazole (29): Yield 53%; mp 214-215 °C; IR (film, cm^{-1}): 3111, 3077, 2917, 2850, 1725, 1626, 1601, 1528, 1515, 1496, 1450, 1435, 1406, 1382, 1365, 1301, 1265, 1245, 1195, 1213, 1173, 1078, 1042; ¹H NMR (400 MHz, $CDCl_3$) δ : 2.36 (s, 3H, CH_3), 4.85 (t, $J = 5.2$ Hz, 2H, NCH_2), 4.95 (t, $J = 5.2$ Hz, 2H, NCH_2), 4.98 (s, 2H, OCH_2), 6.12 (d, $J = 16.1$ Hz, 1H, $CH=CH$), 6.82 (d, $J = 8.0$ Hz, 2H, ArH), 6.92-6.96 (m, 1H, ArH), 7.18-7.22 (m, 2H, ArH), 7.23 (d, $J = 1.5$ Hz, 1H, ArH), 7.25 (s, 1H, ArH), 7.35-7.37 (m, 3H), 7.72 (d, $J = 16.1$ Hz, 1H, $CH=CH$), 8.14 (s, 1H); ¹³C NMR (100 MHz, $CDCl_3$) δ : 21.48, 45.83, 50.00, 61.54, 108.27, 114.57, 121.26, 123.65, 127.71, 129.47, 129.73, 132.01, 135.51, 140.61, 141.50, 145.26, 151.19, 157.92; ESI-MS (m/z): 431.25 [$M + H$]⁺. Anal calcd for $C_{23}H_{22}N_6O_3$: C 64.17, H 5.15, N 19.52. Found: C 64.12, H 5.17, N 19.49.

Acknowledgements

D.S.R. thanks R&D Grant, University of Delhi for financial support. Authors are thankful to CIF-USIC, University of Delhi, India for spectral data.

References

1. E. C. Keen, *Future Microbiol.* 8 (2013) 821-823.
2. J.D. Ospina-Villa, N.Guillén, C. Lopez-Camarillo, J. Soto-Sanchez, E. Ramirez-Moreno, R. Garcia-Vazquez, C.A. Castañon-Sanchez, A. Betanzos, L.A. Marchat, *J. Microbiol.* 55 (2017) 783-791.
3. A.A. Kelsoa, S.D. Goodsona, S. Chavan, A.F. Saya, A. Turchicka, D. Sharma, L.L. Ledforda, E. Rattermana, K. Leskoskea, A.V. King, C.C. Attaway, Y. Bandera, S. H. Foulger, A.V. Mazin, L.A. Temesvari, M.G. Sehorn. *Mol. Biochem. Parasitol.* 210 (2016) 71–84.
4. S.M. Townson, P.F.L. Boreham, P. Upcroft, J.A. Upcroft, *Acta Trop.* 56 (1994) 173-194.
5. S. Moreno, R. Docampo, *Environ. Health Perspect.* 64 (1985) 199–208.
6. P.J. Johnson, *Parasitol. Today* 9 (1993) 183–186.
7. V. Purohit, A.K. Basu, *Chem. Res. Toxicol.* 13 (2000) 673–692.
8. T. Cavas, S. Ergene-Gozukara, *Environ. Toxicol. Pharmacol.* 19 (2005) 107–111.
9. A.F. El-Nahas, I.M. El-Ashmawy, *Basic Clin. Pharmacol. Toxicol.* 94 (2004) 226–231.
10. S. Toumi, M. Hammouda, A. Essid, L. Medimagh, L.B. Slamia, C. Laouani-Kechrid, *Med. Maladies Infect.* 39 (2009) 906–908.
11. S. Becker, P. Hoffman, E.R. Houpt, *Am. J. Trop. Med. Hyg.* 84 (2011) 581–586.
12. S.M. Siddiqui, A. Salahuddin, A. Azam, *Eur. J. Med. Chem.* 49 (2012) 411–416.
13. B. Meunier, *Acc. Chem. Res.* 41 (2008) 69–77.
14. N. Kumar, S. I. Khan, H. Atheaya, R. Mangain, D.S. Rawat, *Eur. J. Med. Chem.* 46 (2011), 2816-2827.
15. S. Manohar, U. C. Rajesh, S.I. Khan, B.L. Tekwani, D.S. Rawat, *ACS Med. Chem. Lett.* 3 (2012), 555-559.
16. F. W. Muregi, A. Ishih, *Drug Dev. Res.* 71 (2010) 20-32.

17. Shaveta, S. Mishra, P. Singh, *Eur. J. Med. Chem.* 124 (2016) 500-536.
18. J.H. Mohammed, *Int. J. Innov. Sci. Eng. Technol.* 2 (2015) 901-904.
19. Beena, N. Kumar, R.K. Rohilla, N. Roy, D.S. Rawat, *Bioorg. Med. Chem. Lett.* 19 (2009) 1396-1398.
20. B. Negi, K.K. Raj, S.M. Siddiqui, D. Ramachandran, A. Azam, D.S. Rawat, *Chem Med Chem.* 9 (2014) 2439-2444.
21. R. Romagnoli, P.G. Baraldi, O. Cruz-Lopez, M.K. Salvador, D. Preti, M.A. Tabrizi, J. Balzarini, A. Canella, E. Fabbri, R. Gambari. *Lett. Drug Design Discov.* 9 (2012) 140-152.
22. M.M. Rubner, C. Holzhauser, P.R. Bohlnder, H.A. Wagenknecht. *Chem. Eur. J.* 18 (2012) 1299-1302.
23. G.A. Hampannavar, R. Karpoornath, M.B.P.M.S. Shaikh, B. Chandrasekaran, *ACS Med. Chem. Lett.* 7 (2016) 686-691.
24. S.L. Zaidi, S. Mittal, M.S. Rajala, F. Avecilla, M. Husain, A. Azam, *Eur. J. Med. Chem.* 98 (2015) 179-189.
25. J. Pais-Morales, A. Betanzos, G. García-Rivera, B. Chávez-Munguía, M. Shibayama, E. Orozco. *PLOS ONE* (2016) 1-23.
26. M. Abid, S. M. Agarwal, A. Azam, *Eur. J. Med. Chem.* 43 (2008) 2035-2039.
27. G. Jeelani, T. Nozaki, *Mol. Biochem. Parasitol.* 206 (2016) 39-45.
28. A. Debnath, D. Parsonage, R.M Andrade, C. He, E.R Cobo, K. Hirata, S. Chen, G. García-Rivera, E. Orozco, M.B. Martínez, S.S Gunatilleke, A.M Barrios, M.R Arkin, L. B Poole, J.H. McKerrow, S.L Reed, *Nature Med.* 18, (2012).
29. D. Leitsch, D. Kolarich, I.B. Wilson, F. Altmann, M. Duchêne, *PLoS Biol.* 5 (2007) e211.
30. M. Abid, S. M. Agarwal, A. Azam, *Eur. J. Med. Chem.* 43 (2008) 2035-2039.
31. C.W. Wright, M.J. O'Neill, J.D. Phillipson, D.C. Warhurst, *Antimicrob. Agents Chemother.* 32 (1988) 1725-1729.
32. D. Parsonage, F Sheng, K. Hirata, A. Debnath, J. H. McKerrow, S. L. Reed, R. Abagyan, L. B. Poole, L. M. Podust. *J. Struct. Biol.* 194 (2016) 180-190.

33. R.M. Andrade, S.L.Reed. *Front. Microbiol.* 6 (2015) 975-980.
34. D. Mustacich, G. Powis, *Biochem. J.* 346, (2000) 1-8.
35. D.G. Arias, E.L. Regner, A.A. Iglesias, S.A. Guerrero. *Biochim. Biophys. Acta* 1820 (2012) 1859-1866.
36. B. Negi, K.K. Raj, S.M. Siddiqui, D. Ramachandran, A. Azam, D.S. Rawat, *Chem Med Chem.* 9 (2014) 2439-2444.
37. A. Salahuddin, S.M. Agarwal, F. Avecilla, A. Azam, *Bioorg. Med. Chem. Lett.* 22 (2012) 5694-5699.
38. L.S. Diamond, D.R. Harlow, C.C. Cunnick, *Trans. R. Soc. Trop. Med. Hyg.* 72 (1978) 431-32.
39. F.D. Gillin, D.S. Reiner, M. Suffness, *Antimicrob. Agents Chemother.* 22 (1982) 342-345.
40. QikProp User Manual Copyright © 2013 Schrödinger, LLC
41. E.M. Duffy, W.L. Jorgensen, *J. Am. Chem. Soc.* 122 (2000) 2878-2888.

Table 1: *In vitro* antiamoebic activity of MTZ-triazole-styryl conjugates

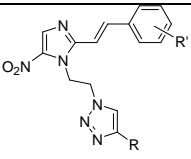
Compound			IC ₅₀ (μ M)
	R	R'	
8	CH ₂ OH	H	1.12 \pm 0.002
9	CH ₂ OH	4-F	0.18 \pm 0.002
10	CH ₂ OH	4-Cl	1.11 \pm 0.002
11	CH ₂ OH	4-Br	1.65 \pm 0.007
12	CH ₂ OH	4-CH ₃	2.13 \pm 0.003
13	CH ₂ OH	4-CH ₂ CH ₃	4.18 \pm 0.001
14	C ₆ H ₅	H	1.35 \pm 0.005
15	C ₆ H ₅	4-F	0.12 \pm 0.004
16	C ₆ H ₅	4-Cl	1.22 \pm 0.013
17	C ₆ H ₅	4-Br	1.77 \pm 0.002
18	C ₆ H ₅	4-CH ₃	2.51 \pm 0.009
19	C ₆ H ₅	4-CH ₂ CH ₃	4.68 \pm 0.001
20	2-pyridyl	H	5.13 \pm 0.005
21	2-pyridyl	4-F	0.13 \pm 0.006
22	2-pyridyl	4-Cl	0.29 \pm 0.008
23	2-pyridyl	4-Br	1.10 \pm 0.005
24	2-pyridyl	4-CH ₃	6.01 \pm 0.004
25	CH ₂ OC ₆ H ₅	H	3.56 \pm 0.005
26	CH ₂ OC ₆ H ₅	4-F	0.28 \pm 0.004
27	CH ₂ OC ₆ H ₅	4-Cl	0.35 \pm 0.006
28	CH ₂ OC ₆ H ₅	4-Br	1.68 \pm 0.009
29	CH ₂ OC ₆ H ₅	4-CH ₃	5.38 \pm 0.013
Ref	MTZ		1.79 \pm 0.001

Table 2: Glide docking energies and XP docking scores of best active molecules along with the reference compound NADP, bound to the binding site of EhTrR.

Compound	Glide Energy (kcal mol⁻¹)	XP GScore (kcal mol⁻¹)
9	-47.60	-6.17
15	-52.48	-6.51
21	-48.12	-6.38
22	-46.85	-5.89
26	-45.98	-6.16
27	-43.84	-5.29
NADP	-73.86	-9.43

Table 3: Prediction of Lipinski's 'rule of 5' for the active test compounds

Comp.	#rotor (0 – 15)	mol_MW (< 500 amu)	donorHB (< 5)	accptHB (< 10)	QPlogPo/w (- 2.0 to 6.5)	Rule of Five (< 4)
8	9	340.34	1	6.7	1.986	0
9	9	358.33	1	6.7	2.212	0
10	9	374.79	1	6.7	2.465	0
11	9	419.24	1	6.7	2.703	0
12	9	354.37	1	6.7	2.285	0
13	10	368.39	1	6.7	2.627	0
14	7	386.41	0	5	3.751	0
15	7	404.40	0	5	4.397	0
16	7	420.86	0	5	4.124	0
17	7	465.31	0	5	4.184	0
18	7	400.44	0	5	4.484	0
19	8	414.47	0	5	4.36	0
20	7	387.4	0	6	3.729	0
21	7	405.39	0	6	3.783	0
22	7	421.85	0	6	4.04	0
23	7	466.30	0	6	3.437	0
24	7	401.43	0	6	3.873	0
25	10	416.44	0	5.75	4.677	0
26	10	434.43	0	5.75	4.26	0
27	10	450.88	0	5.75	5.159	1
28	10	495.33	0	5.75	4.378	0
29	10	430.47	0	5.75	4.178	0
MTZ	4	171.16	1	4.2	-0.019	0

Table 4: Calculated ADMET properties

Comp.	#rotor (0-15)	QPlogS (-6.5- 0.5)	QPlogHERG (concern below -5)	QPPCaco (<25 poor, >500 great)	QPlogBB (-3.0-1.2)	QPPMDCK (<25 poor >500 great)	QPlogKhsa (-1.5to1.5)	Percent Human Oral Absorption (>80% high, <25% poor)	PSA (7.0 – 200.0)
8	9	-3.045	-5.224	139.108	-1.778	58.67	-0.225	76.934	113.402
9	9	-3.386	-5.097	140.244	-1.674	107.139	-0.189	78.325	113.318
10	9	-3.748	-5.153	140.451	-1.641	146.41	-0.12	79.814	113.319
11	9	-4.226	-5.612	152.481	-1.686	172.042	-0.059	81.849	113.311
12	9	-3.595	-5.18	139.206	-1.838	58.715	-0.077	78.689	113.403
13	10	-3.949	-5.299	139.338	-1.947	58.775	0.027	80.703	113.405
14	7	-4.143	-5.523	273.689	-1.317	121.925	0.355	92.531	91.721
15	7	-5.422	-6.421	345.115	-1.271	283.558	0.517	100	89.478
16	7	-4.595	-5.294	275.654	-1.173	250.827	0.448	94.767	91.635
17	7	-4.664	-5.284	276.423	-1.16	268.334	0.467	95.145	91.6
18	7	-5.653	-6.47	347.611	-1.415	157.88	0.643	100	89.495
19	8	-4.839	-5.396	276.429	-1.413	123.245	0.616	96.171	91.646
20	7	-4.954	-6.906	268.858	-1.563	119.6	0.258	92.266	101.624
21	7	-4.833	-6.362	288.645	-1.352	233.764	0.224	93.129	100.844
22	7	-5.21	-6.395	287.732	-1.313	317.852	0.302	94.61	100.838
23	7	-3.629	-4.863	319.495	-1.042	320.827	0.075	91.895	99.782
24	7	-5.075	-6.417	289.078	-1.501	129.351	0.353	93.669	100.854
25	10	-5.535	-7.413	515.31	-1.503	241.618	0.45	100	97.815
26	10	-4.542	-5.864	278.917	-1.471	214.666	0.347	95.658	98.848
27	10	-6.345	-7.348	477.266	-1.405	549.24	0.579	92.14	98.796
28	10	-4.78	-5.919	269.318	-1.472	247.833	0.384	96.075	98.97
29	10	-4.527	-5.838	270.275	-1.604	120.282	0.398	94.935	98.95
MTZ	4	-1.25	-3.156	259.68	-1.001	115.193	-0.689	70.045	81.489

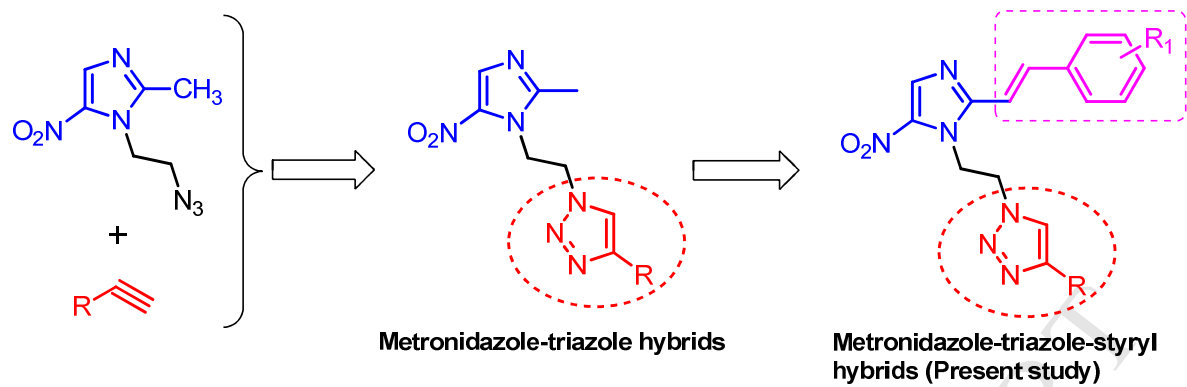


Fig. 1: Design strategy of the novel metronidazole-triazole-styryl hybrids

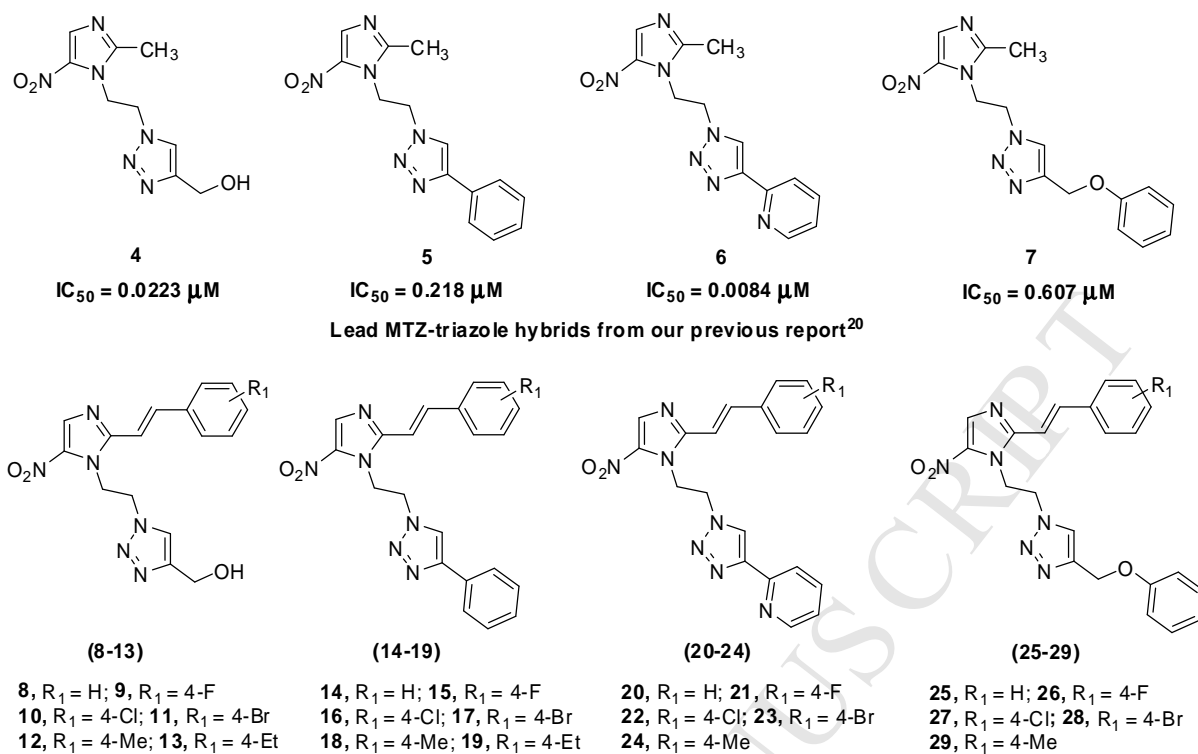


Fig. 2: Structures of MTZ-triazole-styryl hybrids

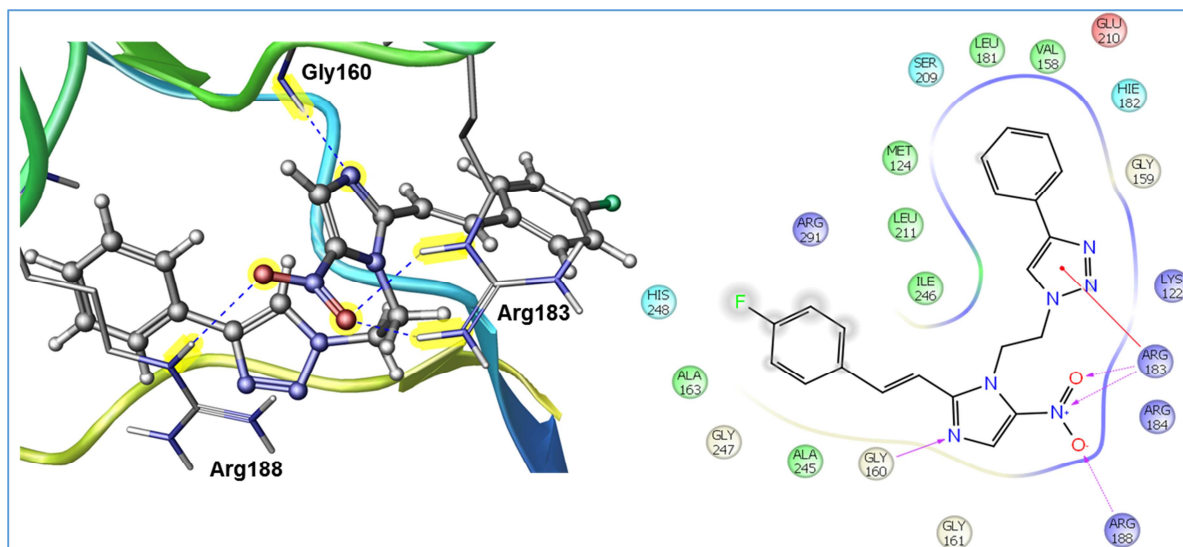


Fig. 3: 2D and 3D docking pose showing interaction for compound **15** in the binding site of EHTrR.

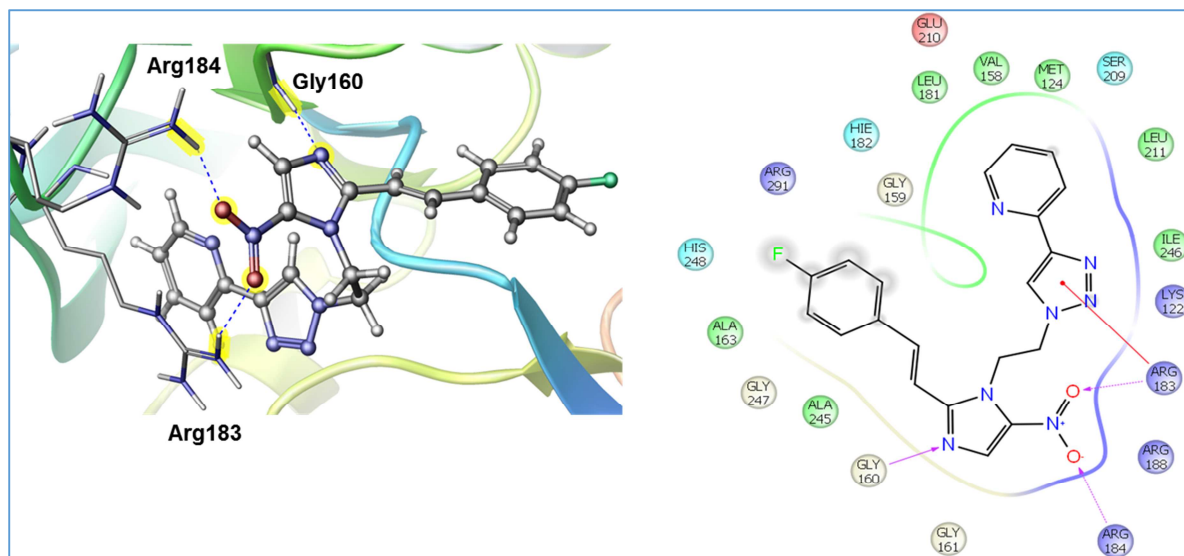
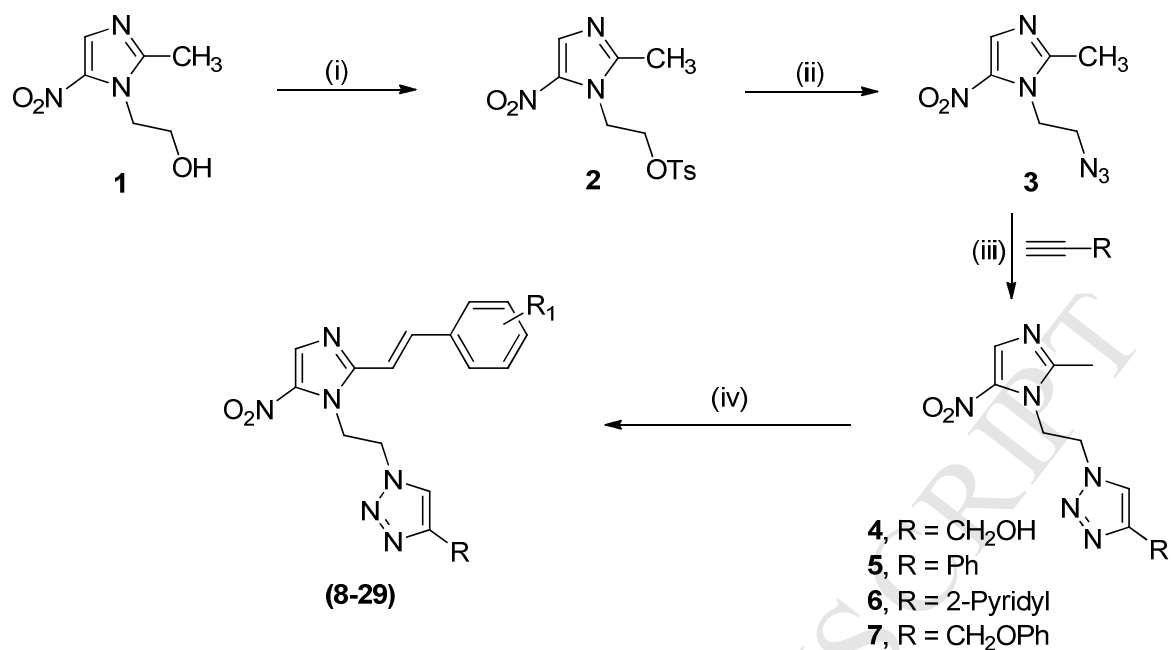


Fig. 4: 2D and 3D docking pose showing interaction for compound **21** in the binding site of EHTrR.



Scheme 1: Reagents and conditions: (i) p-TsCl, Pyridine, RT, 12 h; (ii) NaN₃, DMF at 0°C then 70–80 °C for 1 h; (iii) t-BuOH : H₂O (1:1) , Sodium ascorbate, CuSO₄·5H₂O; (iv) Substituted benzaldehydes, DMSO, Dry MeOH, NaOMe, 40 °C, 12 h

Highlights

- Synthesis of novel metronidazole-triazole-styryl hybrids.
- Antiamoebic activity against HM1: IMSS strain of *Entamoeba histolytica*.
- Investigated molecular docking studies with EhTrR protein and ADMET properties.

ACCEPTED MANUSCRIPT